

ROCOCO - A Zero Dispersion Algorithm for Calculating Wake Potentials*

Robert Hampel**, Wolfgang F.O. Müller, Thomas Weiland

Technische Universität Darmstadt, Institut fuer Theorie Elektromagnetischer Felder (TEMF)

Schlossgartenstr. 8, 64289 Darmstadt, Germany

Abstract

Wake fields are a limiting factor due to their collective effects. In colliders and high energy accelerators used in FEL projects short bunches excite high frequency fields which make the computation of near range wake fields difficult due to resolution problems. Additionally, the length of modern accelerating structures limit the various abilities of codes such as TBCI or MAFIA[1] due to limited memory. Both limiting factors, i.e. short bunches and length of accelerating structures – a multi-scale problem, can be dealt with in the following way. Using zero dispersion directions of the leap-frog update scheme on a usual Cartesian grid leads to a decrease of the overall dispersion which usually arises by having discrete field values. Combined with a conformal modeling technique allowing for simulations using the full time step given by the Courant criterion a moving window technique can be applied. Thus, simulations of short bunches in long structures are possible – dispersion and memory problems have been avoided. Results for common structures of accelerator physics – such as collimators, tapers and the TESLA nine cell structure are shown.

INTRODUCTION

In this work ROCOCO (Rotated mesh and conformal code) is presented. The zero dispersion algorithm uses a new discretization scheme based on a rotated mesh combined with the established USC scheme [2] scheme and a moving window technique. The advantage of an explicit algorithm is joined with the zero dispersion along the beam's propagation direction.

The dispersion properties of a numerical algorithm are usually investigated by a von Neumann dispersion analysis. This analysis yields a numerical dispersion depending on the directions in a Cartesian mesh.

The well known leap-frog update scheme has maximum dispersion along the edges of a mesh cell (Fig.1). In contrast to this it has zero dispersion along directions which are aligned to the diagonals of the mesh cell, i.e. the diagonal of a square (2D) or the diagonal of a hexaeder (3D).

PROPERTIES OF THE ALGORITHM

The basic idea of ROCOCO (2D) is to utilize the dispersion-less directions provided by the time integration scheme. One of these dispersion-less directions is aligned

* This work was partially funded by EUROTeV (RIDS-011899) and DESY Hamburg.

**hampel@temf.tu-darmstadt.de

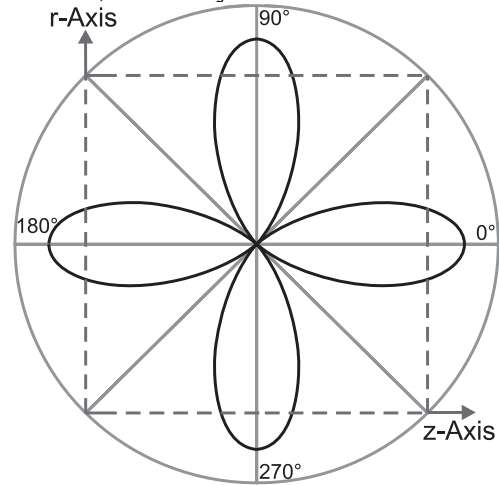


Figure 1: Dispersion error (qualitative) versus angle for the leap-frog update scheme. A mesh cell is indicated by the dashed lines.

with the bunch's direction of motion by rotating the mesh by an angle of 45°.

Building the Mesh and Discretization

Starting from a rotated mesh, the rest of the algorithm is realized straight forward. Maxwell's equations for a circular cylindrical symmetric structure and symmetric fields ($m = 0$)

$$\partial_t h_\phi = -\frac{1}{\mu_\phi} (\partial_z e_r - \partial_r e_z) \quad (1a)$$

$$\partial_t e_r = \frac{1}{\epsilon_r} (-\partial_z h_\phi) \quad (1b)$$

$$\partial_t e_z = \frac{1}{\epsilon_z} \frac{1}{r} \partial_r (r \cdot h_\phi) + j_z \quad (1c)$$

are discretized on this rotated mesh. Considering a rotation of the two base vectors \vec{e}_r and \vec{e}_z by 45° yields two new base vectors \vec{e}_u and \vec{e}_v . This is shown in the sketch in Fig. 2.

In order to advance a charge distribution moving at the speed of light c_0 by one mesh step Δz in a standard Cartesian mesh the time step Δt has to be chosen according to $\Delta t = \frac{\Delta z}{c_0}$. This time step will lead to instabilities because it violates the Courant criterion $\Delta t \leq \frac{\Delta z}{c_0 \cdot \sqrt{2}}$. The rotation of the mesh enables one to meet the Courant criterion exactly. Referring to the new coordinates the time step needed for an advance of one mesh step in the beam direction becomes

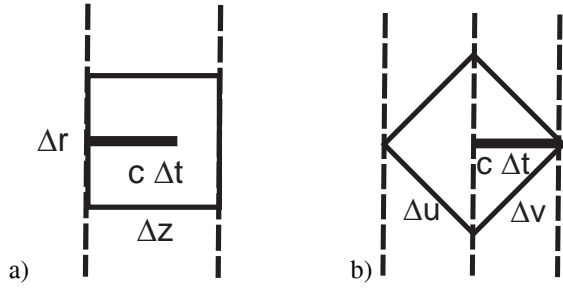


Figure 2: Standard mesh cell (a), rotated mesh cell (b)

$\Delta t = \frac{\Delta v}{c_0 \cdot \sqrt{2}}$ which is identical to the upper limit given by the Courant criterion.

The change from (r, z) to (u, v) can be applied to the set of equations 1a-1c obtaining

$$\partial_t h_\phi = -\frac{1}{\mu_\phi} (\partial_v e_u - \partial_u e_v) \quad (2a)$$

$$\partial_t e_u = \frac{1}{\epsilon_u} \frac{1}{r} (-\partial_v (r \cdot h_\phi)) + j_u \quad (2b)$$

$$\partial_t e_v = \frac{1}{\epsilon_v} \frac{1}{r} (\partial_u (r \cdot h_\phi)) + j_v \quad (2c)$$

Excitation

In a next step the exciting fields of a bunch have to be introduced. Gaussian shaped bunches have been used in the following examples. Applying currents according to the equations 2b-2c would lead to a full field formulation, i.e. the total field is involved in the time update scheme. A better way to implement the excitation is to apply a scattered field approach [3]. Fulfilling the boundary conditions for the total fields $total = (s)cattered + (e)xciting$ on the surface of the structure, allows for a separation of the scattered and the exciting fields (equations 3a-3c). The excited fields are determined only once. They appear as an additive driving term in equations 3a-3c and therefore they do not experience numerical dispersion. Thus, only the scattered fields take part in the time update scheme and noise is reduced.

$$\partial_t h_\phi^s = -\frac{1}{\mu_\phi} (\partial_v e_u^s - \partial_u e_v^s) - \left(1 - \frac{\mu_0}{\mu_\phi}\right) \partial_t h_\phi^0 \quad (3a)$$

$$\partial_t e_u^s = \frac{1}{\epsilon_u} \frac{1}{r} (-\partial_v (r \cdot h_\phi^s)) - \left(1 - \frac{\epsilon_0}{\epsilon_u}\right) \partial_t e_u^0 \quad (3b)$$

$$\partial_t e_v^s = \frac{1}{\epsilon_v} \frac{1}{r} (\partial_u (r \cdot h_\phi^s)) - \left(1 - \frac{\epsilon_0}{\epsilon_v}\right) \partial_t e_v^0 \quad (3c)$$

Furthermore, in contrast to a current excitation on axis, the excited fields only have to travel from the surface to the axis. This minimizes a source of additional dispersion errors. The discretization of the set of equations 3a-3c is done using the *Finite Integration Technique* [4, 5].

Moving Window Technique

Since the simulations are done using an ultra relativistic bunch, i.e. $v = c_0$, no fields can travel in front of the bunch. This enables one to use a moving window technique [6] to minimize memory needs. Only the region of the structure covered by the bunch has to be stored in memory when calculating near range wake fields. Therefore, the physical length of the structure to be simulated, is not limited by memory anymore.

Finally, the approximation of the surface of the structure is done. Many conformal techniques like PFC [7, 8] reduce the time step locally compared to the maximum time step given by the Courant limit. The USC uses an approach of enlarging a partially filled cell by interpolations incorporating neighboring cells. A time step reduction is not needed any more. This conformal scheme can be combined with the rotated mesh approach.

The assembly and manipulating of the material matrices can be done on the fly, i.e. only on the front side of the moving window.

Indirect Integration

In order to obtain the wake potential from the wake fields one has to integrate E_z along the structure's axis. This integral has limits to infinity. Therefore it is not possible to calculate the wake potential by a direct integration on the axis. One has to stop the integration at a finite position which leads to inaccurate results. Using an indirect integration technique [9] enables one to perform the integration in between finite limits. Additionally, the technique allows for integrating along arbitrary paths [10]. Thus, structures such as tapers and collimators can be simulated.

EXAMPLES AND RESULTS

For verification purposes different structures are simulated. First a hypothetical structure of 20 TESLA-like cells is simulated in order to check for the absence of accumulating errors in long time simulations. The next two examples are more practical ones. Secondly a small part of the PITZ setup [11] is simulated and thirdly a cylindrically symmetric collimator is investigated.

20 Cell TESLA-like Structure

This hypothetical structure is used instead of a TESLA 9 cell structure to investigate the occurrence of accumulating dispersion errors. The results obtained using ROCOCO are compared to simulations done with ECHO. The parameters of the simulation are $\sigma = 1$ mm and the charge of the bunch is $q = 1$ nC. Five mesh cell diagonals are used to resolve one σ . The resolution used in ECHO is of a comparable value. Both resolutions do not match exactly because the edge of a cell (ECHO) has to be compared with the diagonal of a cell (ROCOCO) which is larger by a factor of $\sqrt{2}$.

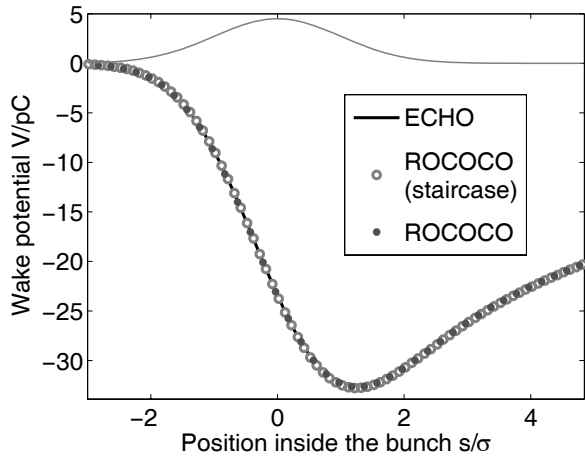


Figure 3: ECHO, ROCOCO (staircase), ROCOCO – $\sigma = 1$ mm, 5 cell diagonals per σ . The driving Gaussian charge distribution is shown qualitatively.

In Fig. 3 three results are shown. The black line represents the ECHO result. Grey dots and gray circles indicate the results of ROCOCO. The dots show the conformal result and the circles show the result using a staircase approximation of the surface. To emphasize the conformal approximation of the surface the near range wake potential is shown zoomed in Fig. 4.

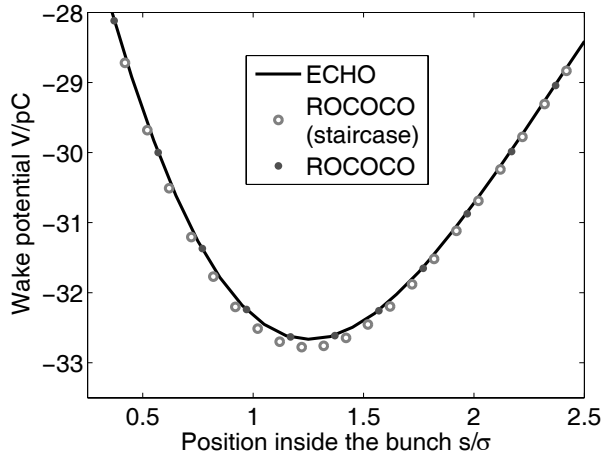


Figure 4: ECHO, ROCOCO (staircase), ROCOCO – $\sigma = 1$ mm, 5 cell diagonals per σ . The markers (gray circles and gray dots) are the same as in the previous figure (Fig. 3).

It is obvious that the staircase approximation of the surface leads to a less accurate result as the two results obtained using a conformal approximation of the structure.

Step in the PITZ Gun

In the setup of the PITZ gun a change of the radii of the inner tube of the coupler antenna and the following beam

tube is present. This step is simulated and a study to investigate the effect of a tapering is done. Basically the radius changes from 16.75 mm to 18.5 mm.

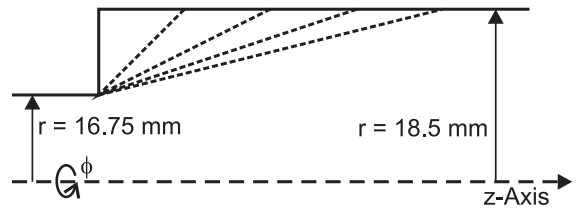


Figure 5: Step in the PITZ gun. Angles of the tapers are not to scale.

One simulation is done for a step, i.e. the radius jumps from one value to the other one. Four simulations follow using different angles for a taper.

The bunch charge q is 1 nC and the bunch has a σ of 2.5 mm. For the angle of the taper the four angles 45° , 20° , 8° and 4° are used.

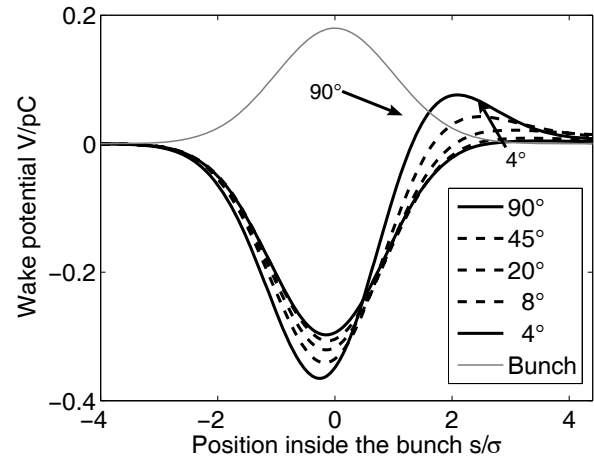


Figure 6: Wake potential of a tapered step in the PITZ gun. The Gaussian bunch is shown qualitatively.

One can observe that the wake potential does not vanish for an infinitely smooth tapering. This is easily explained by an energy consideration. Before passing the step or the taper, the fields of the bunch have an energy density which gives an amount of energy being stored in the inner tube of the coupler antenna. Far behind the step or the taper, the amount of energy stored in the beam tube is larger because the radius and hence the volume is larger. The difference of these energies corresponds exactly to the loss of energy of the bunch. Tapering reduces the impact on the bunch but it cannot switch off any effect of a change in the radius.

In a different approach the wake potential for an infinitely small angle can be calculated analytically. One has to carry out the integration of the electromagnetic fields of the bunch along a radial path

$$\begin{aligned} \lim_{\alpha \rightarrow 0} W_{||}(s, \alpha) &= -\frac{1}{q} \int_C (E_r + c_0 B_\phi) dr \\ &= \frac{1}{\pi \epsilon_0} \ln \left(\frac{r_{\text{initial}}}{r_{\text{final}}} \right) \lambda(s). \end{aligned} \quad (4)$$

The wake potential has the same shape as the charge distribution $\lambda(s)$ which is nearly fulfilled by the graph corresponding to a tapering angle of 4° in Fig. 6. Furthermore equation 4 shows an agreement to the additive term derived in [10]. This term arises by changing from total to scattered fields in the integration of the wake potential. Thus, demanding the solution of the same integral as in equation 4.

Collimator

The last simulation deals with a collimator. It is circular cylindrical symmetric but it is not symmetric in the longitudinal direction, i.e. the incoming angle $\alpha = 3.18^\circ$ is slightly different from the outgoing angle $\beta = 2.86^\circ$. The two radii are $R = 0.01$ m and $r = 0.005$ m.

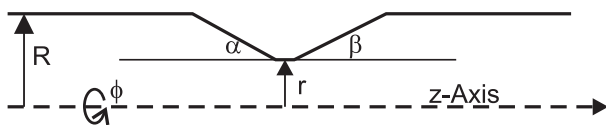


Figure 7: Sketch of the collimator

The σ of the Gaussian bunch is 0.5 mm and the bunch charge is again $q = 1$ nC. The results of ECHO and ROCOCO are compared. Using comparable resolutions as mentioned above one obtains Fig. 8.

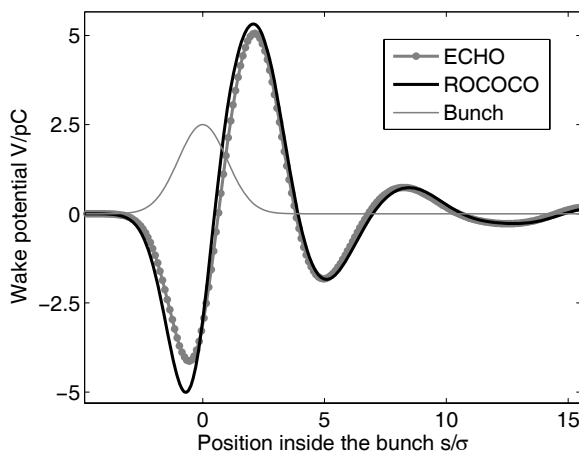


Figure 8: Wake potential of the collimator shown in Fig. 7. Results from ECHO and ROCOCO are compared. The Gaussian bunch is shown qualitatively.

The result of ROCOCO gives a quite good agreement for the far range wake potential compared to ECHO's result. Obviously the near range wake potential given by ROCOCO and ECHO show deviations. The discrepancy of the two results is still a point of ongoing investigations.

CONCLUSIONS

In this paper an algorithm is described which allows for low dispersive simulations along one direction in a rotated mesh. The excitation of the fields is implemented by a scattered fields approach. Due to a moving window technique wake potentials of various long structures and discontinuities can be computed. An accumulation of dispersion errors is not observed. Realistic structures such as a step in the PITZ gun or a collimator have been investigated.

However, there are some minor differences in the result for the collimator. ROCOCO's and ECHO's result do not match in the near range wake potential. The reason for that is an object of further work to do.

REFERENCES

- [1] CST GmbH, Bad Nauheimer Str. 19, 64289 Darmstadt
- [2] I. Zagorodnov, R. Schuhmann and T. Weiland, "A uniformly stable conformal FDTD-method in Cartesian grids", International Journal of Numerical Modelling, Vol. 16 (2003), pp. 127-141.
- [3] M. Dehler, "Numerical Wake Calculations using an Equivalence Principle", Proceedings of the Particle Accelerators Conference, 1995, Vol. 49, pp. 105-116.
- [4] T. Weiland, "A discretization method for the solution of Maxwell's equations for six component fields", Electronics and Communications (AEÜ), Vol. 31 (1977), p. 116.
- [5] T. Weiland, "On the Numerical Solution of Maxwell's Equations and Applications in Accelerator Physics", Particle Accelerators Vol. 15 (1984), pp. 245-292.
- [6] K. Bane, T. Weiland, "Wake Force Computation in the Time Domain for Long Structures", Proceedings of the 12th International Conference on High Energy Accelerators, Chicago, 1983, pp. 314-316.
- [7] S. Dey, R. Mitra, "A locally conformal finite-difference time-domain (FDTD) algorithm for modeling three-dimensional perfectly conducting objects", IEEE Microwave and Guided Wave Letters 1997; 7(9):273-275.
- [8] B. Krietenstein, R. Schuhmann, P. Thoma, T. Weiland, "The Perfect Boundary Approximation Technique Facing the Big Challenge of High Precision Field Computation", Proceedings of the XIX International Linear Accelerator Conference (LINAC 98), Chicago, USA, 1998, pp. 860-862.
- [9] T. Weiland, "Comment on Wake Field Computation in Time Domain", Nuclear Instruments and Methods (NIM), Vol. 216 (1983), pp. 31-34.
- [10] O. Napoly, Y.H. Chin, B. Zotter, "A Generalized Method for Calculating Wake Potentials", Nuclear Instr. and Methods in Phys. Research, Sec. A, Vol. 334 (1993), pp. 255-265.
- [11] A. Oppelt, "The Photo Injector Test Facility at DESY Zeuthen: Results of the First Phase", LINAC 2004.